A Reversible Structural Interconversion Involving $[M(H_2pdc)_2(H_2O)_2]\cdot 2H_2O$ ($M = Mn, Fe, Co, Ni, Zn$, H_3pdc = 3,5-pyrazoledicarboxylic acid) and the Role of A Reactive Intermediate $[Co(H_2pdc)_2]$

Long Pan, Nancy Ching, Xiaoying Huang, and Jing Li*[a]

Abstract: A new type of hydrogen bonded networks $[M(H_2pdc)_2(H_2O)_2]\cdot 2H_2O$ [M = Mn (**1**), Fe (**2**), Co (**3**), Ni (**4**), Zn (**5**); H_3pdc = 3,5-pyrazoledicarboxylic acid] have been synthesized via hydrothermal reactions and their structures have been characterized. Upon a cooling-heating cycle, these compounds undergo a reversible structural interconversion process via hydration-dehydration: $[M(H_2pdc)_2(H_2O)_2]\cdot 2H_2O \underset{+4H_2O}{\overset{-4H_2O}{\rightleftharpoons}} [M(H_2pdc)_2]$. The process is associated with distinct color changes. The dehydrated $[M(H_2pdc)_2]$ (M = Mn, Fe, Co, Ni, and Zn) are amorphous and highly reactive. Further chemical reactions of these reactive intermediates show that they may act as effective precursors towards assembly of new supramolecular compounds that may otherwise be inaccessible by other synthetic routes. An interesting structure containing an "open-box" molecule $[Co_4(Hpdc)_4(py)_{12}]\cdot 4py\cdot 2H_2O\cdot 2CH_3OH$ (**6**) (py = pyridine) has been isolated by using dehydrated $[Co(H_2pdc)_2]$ as the precursor, and its crystal structure has been analyzed. Crystal data for **1**–**6**: monoclinic, space group $P2_1/c$ and $Z = 2$ with $a = 10.186(2)$, $b = 12.473(2)$, $c = 6.831(1)$ Å, $\beta = 108.80(3)^\circ$ (**1**); $a = 9.896(2)$, $b = 12.402(2)$, $c = 6.810(1)$ Å, $\beta = 108.15(3)^\circ$ (**2**); $a = 9.981(2)$, $b = 12.426(2)$, $c = 6.807(1)$ Å, $\beta = 108.23(3)^\circ$ (**3**); $a = 9.896(2)$, $b = 12.402(2)$, $c = 6.810(1)$ Å, $\beta = 108.15(3)^\circ$ (**4**); $a = 10.001(2)$, $b = 12.430(2)$, $c = 6.834(1)$ Å, $\beta = 108.32(3)^\circ$ (**5**); $a = 9.9617(1)$, $b = 18.5080(2)$, $c = 28.4786(3)$ Å, $\beta = 93.076(1)^\circ$ (**6**).

Keywords: carboxylate ligands · hydrogen bonds · self-assembly · structure elucidation · supramolecular chemistry

Introduction

Recent interest in the development of supramolecular networks organized and held by means of intermolecular interactions, such as hydrogen bonding or π–π interactions, has attracted tremendous attention due to their fascinating crystal structures, electronic and optical properties, and potential applications as molecular devices such as sensors and indicators.[1] Hydrogen bonding, as the strongest and most directional intermolecular force, has been intensively investigated in organic crystalline solids,[2] but is relatively unexplored in the coordination complexes.[3] In the search for new functional hydrogen-bonded metal coordination network structures, we have investigated a divalent metal 3,5-pyrazoledicarboxylate system involving Groups 7–10 and Group 12 metal centers. The ligand, 3,5-pyrazoledicarboxylic acid (H_3pdc), known both as a multiple proton donor and acceptor, can use its carboxylate oxygen and pyrazole nitrogen atoms, which are highly accessible to metals, to form both monodentate and/or multidentate M–O and M–N bonds. The coordinated structural motifs thus generated can then readily form hydrogen-bonded networks.[4–5]

To date, the majority of known supramolecular assemblies are synthesized by direct reactions of metal salts with various ligands. Recently, a "secondary building block" approach introduces an alternative route that uses cluster molecules as reaction precursors.[6–7] Due to their low solubility in most common organic or inorganic solvents, very few examples are known in which coordination compounds themselves are employed as precursors.[5a] However, when a ligand (or an ancillary solvent molecule) is removed from a coordination complex, the metal coordination in the so-formed intermediate species becomes unsaturated, and the uncoordinated site becomes highly reactive. These intermediate species can then be used as reactive precursors for further reactions. Such reactions often lead to new structures that retain certain features of the intermediate species and that may not be accessible by other routes. Herein, we report the hydrothermal synthesis and crystal structure of a new type of hydrogen-bonded network $[M(H_2pdc)_2(H_2O)_2]\cdot 2H_2O$, M =

---

[a] Prof. J. Li, Dr. L. Pan, N. Ching, Dr. X. Huang
Department of Chemistry, Rutgers University
Camden, NJ 08102 (USA)
Fax: (+1) 856-225-6506
E-mail: jingli@crab.rutgers.edu

Mn (**1**), Fe (**2**), Co (**3**), Ni (**4**) and Zn (**5**), their reversible structural interconversion associated with color change, and the reactions of the dehydrated Co intermediate $[Co(H_2pdc)_2]$ with pyridine. A novel compound, $[Co_4(Hpdc)_4(py)_{12}]\cdot 4py\cdot 2H_2O\cdot 2CH_3OH$ (**6**), was produced from these reactions. Attempts of synthesizing **6** by direct reactions of metal salts and ligands were not successful.

Results and Discussion

The crystal structures of $[M(H_2pdc)_2(H_2O)_2]\cdot 2H_2O$ (M = Mn, Fe, Co, Ni, Zn): Five new compounds were synthesized by stoichiometric mixing of divalent metal salts $M(NO_3)_2/M'Cl_2$ (M = Co, Ni, Zn; M′ = Mn), H_3pdc, and H_2O. The reactions were carried out in 23 mL acid-digestion bombs at 150 °C for three days. For the iron compound, $Fe(NH_4)_2(SO_4)_2$ was used since $FeCl_2/Fe(NO_3)_2$ as starting material resulted in an unknown powder. Low pHs were observed in all reactions (final pH = 1.5 – 2). Single-phase samples were obtained for compounds **1**, and **3** – **5** as confirmed by powder X-ray diffraction (PXRD) analysis, although most yields were not particularly high due to the complex redox process involved in the reactions.[8] Orange-yellowish, beige, and powder blue polycrystalline samples were isolated for Fe, Co, and Ni phases, respectively. The Mn and Zn compounds were colorless.

Single-crystal X-ray diffraction analysis on selected crystals showed that all five compounds **1** – **5** are isostructural, and crystallize in the monoclinic crystal system, space group $P2_1/c$ (No. 14). The structure contains undulating sheets of $[M(H_2pdc)_2(H_2O)_2]\cdot 2H_2O$. Figure 1 shows a view of structure **3**. Within each layer, the metal atoms are located at the inversion center and are six-coordinate. Each metal center is bonded to two 3,5-pyrazoledicarboxylate ions at equatorial positions through the chelating carboxylate oxygen O1 and its adjacent pyrazole nitrogen N1, with the Co–O and Co–N bond lengths of 2.1062(19) and 2.108(2) Å. These bond lengths are consistent with those found in comparable structures.[9] In addition, each metal center is also coordinated to two water molecules at apical positions with a Co–O bond length of 2.058(2) Å, which is stronger compared to those in Cu – pdc compounds of a similar structure.[10] The two H_2pdc^- ions are attached to the metal centers in a *trans* manner, each forming a stable five-membered ring with acute O-Co-N angles (76.91(8)°).

The corresponding bond lengths of metal with carboxylic oxygen atoms (Mn–O = 2.179(3), Fe–O = 2.161(2), Ni–O = 2.079(3), Zn–O = 2.1202(19) Å) and with nitrogen atoms (Mn–N = 2.207(4), Fe–N = 2.139(3), Ni–N = 2.041(4), Zn–N = 2.100(2) Å) fall in the same range as analogous chelating M–O and M–N bonds.[11] All C–O, C–C, and N–N bonds, and pyrazole ring angles in the H_2pdc^- (or pdc) ligand are consistent with those reported previously.[4] As shown in Figure 1, a two-dimensional network with a rare parquet (basket weave) pattern[12] is formed through strong hydrogen bonds between the carboxylate oxygen (O2) and hydrogen (H1) of the neighboring 3,5-pyrazoledicarboxylate ions ($O4-H1\cdots O2^{ii}$ = 2.529(3) Å). The building-block of the parquet is a 36-membered H-bonded ring known as graph set $R_4^4(36)$.[13] Two solvated water molecules are found inside each ring and are held in place through three types of hydrogen bonds; one formed by its oxygen atom with a protonated pyrazole nitrogen atom ($N2-H2\cdots O6$ = 2.707(3) Å), and the other two by the two hydrogen atoms with two different carboxylic oxygen atoms to give $O6-H4\cdots O3^{ii}$ = 2.919(3) Å and $O6-H5\cdots O1^{i}$ = 2.832(3) Å. The interlayer interactions are through hydrogen bonding between the coordinated water O5 in one sheet and the 3,5-pyrazoledicarboxylic oxygen atoms $O2^{iii}$, $O3^{iv}$ in the adjacent sheet with two hydrogen bonds $O5-H2\cdots O2^{iii}$ = 2.728(3) and $O5-H3\cdots O3^{iv}$ = 2.855(3) Å. This gives rise to a hydrogen-bonded, undulating, three-dimensional structure (Figure 2). Selected bond lengths and angles for all structures are given in Tables 1 and 2. The hydrogen bonds are listed in Table 3.

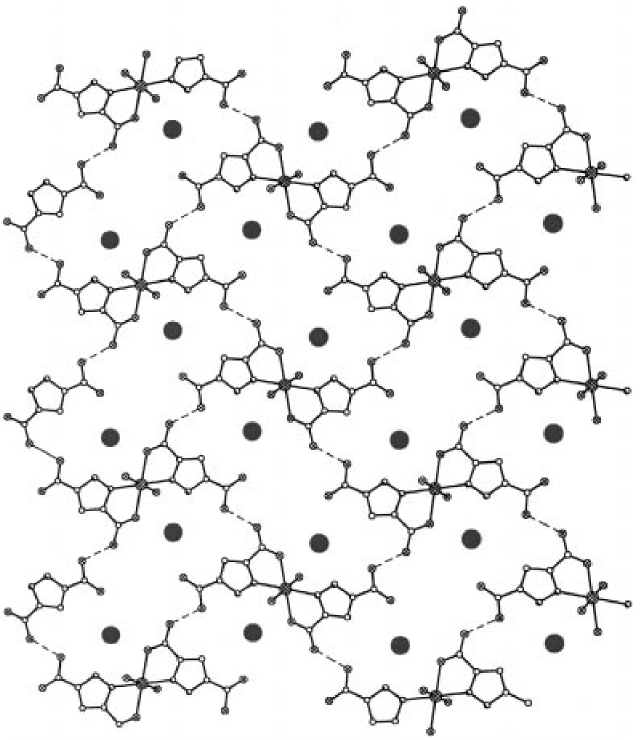

Figure 1. View of the basket-weave-like, two-dimensional hydrogen-bonded network of $[M(H_2pdc)_2(H_2O)_2]\cdot 2H_2O$, M = Mn (**1**), Fe (**2**), Co (**3**), Ni (**4**), and Zn (**5**) along the *c* axis. Large cross-shaded circles are metal atoms, small cross-shaded, open, and partially shaded circles are O, C, and N atoms, respectively. Large solid circles represent the two solvated water molecules. Hydrogen bonds are indicated by dotted lines.

The reversible structural interconversion: To assess the thermal stability of compounds **1** – **5** and their structural variation as a function of the temperature, thermogravimetric analyses (TGA) were performed on single-phase polycrystalline samples of **1** and **3** – **5**. For example, the onset of the weight loss of the four (two solvated and two coordinated) water molecules in **3** occurred at about 90 °C and completed at 220 °C (obsd 16.4 %, calcd 16.3 %). The loss of the 3,5-pyrazoledicarboxylate ligands began at about 250 °C. PXRD on the final residues at 800 °C indicated that the remainder of the sample was elemental Co with some minor cobalt oxide.

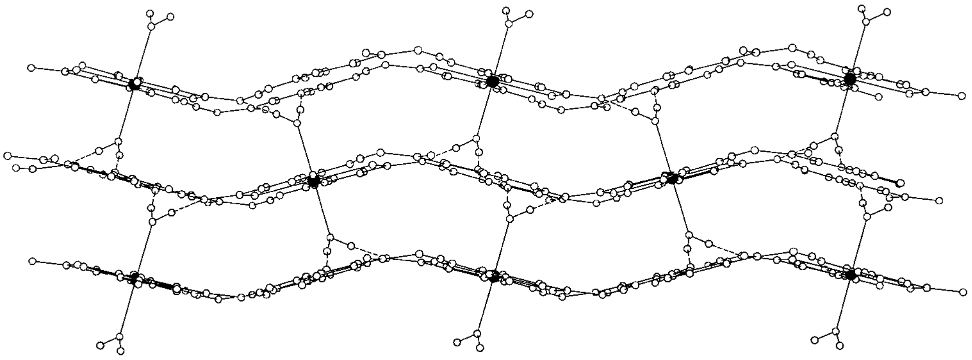

Figure 2. View along the *a* axis showing hydrogen-bonded (wave-like) three-dimensional structure. The interlayer interactions are through hydrogen bonding between the coordinated water molecules (at apical positions) in one layer and the 3,5-pyrazoledicarboxylate ions in the adjacent layer.

Table 1. Selected bond lengths [Å] and angles [°] for **1**, **2**, **3**, **4**, and **5**.

	1(Mn)	**2**(Fe)	**3**(Co)	**4**(Ni)	**5**(Zn)
M−O5^{i}	2.152(4)	2.089(3)	2.058(2)	2.047(4)	2.096(2)
M−O5	2.152(4)	2.089(3)	2.058(2)	2.047(4)	2.096(2)
M−O1	2.179(3)	2.161(2)	2.1062(19)	2.079(3)	2.1202(19)
M−O1^{i}	2.179(3)	2.161(2)	2.1062(19)	2.079(3)	2.1202(19)
M−N1	2.207(4)	2.139(3)	2.108(2)	2.041(4)	2.100(2)
M−N1^{i}	2.207(4)	2.139(3)	2.108(2)	2.041(4)	2.100(2)
O1−C1	1.257(5)	1.247(4)	1.263(3)	1.248(6)	1.249(3)
O2−C1	1.250(5)	1.261(4)	1.251(3)	1.262(6)	1.257(3)
O3−C5	1.209(5)	1.204(4)	1.207(3)	1.196(6)	1.208(3)
O4−C5	1.288(6)	1.302(4)	1.301(3)	1.315(6)	1.302(3)
N1−C2	1.333(6)	1.341(4)	1.336(3)	1.351(6)	1.336(3)
N1−N2	1.338(5)	1.326(4)	1.327(3)	1.325(5)	1.328(3)
N2−C4	1.351(6)	1.351(4)	1.351(3)	1.340(6)	1.350(3)
C1−C2	1.489(6)	1.486(5)	1.489(4)	1.494(6)	1.492(4)
C2−C3	1.399(6)	1.389(5)	1.400(4)	1.386(6)	1.394(4)
C3−C4	1.378(6)	1.378(5)	1.370(4)	1.385(6)	1.371(4)
C4−C5	1.473(6)	1.469(5)	1.485(4)	1.461(6)	1.477(4)
O5^{i}-M-O5	180.0	180.0	180.0	180.0	180.0
O5^{i}-M-N1^{i}	91.57(15)	91.00(11)	90.89(9)	90.29(16)	90.89(9)
O5-M-N1^{i}	88.43(15)	89.00(11)	89.11(9)	89.71(16)	89.11(9)
O5^{i}-M-N1	88.43(15)	89.00(11)	89.11(9)	89.71(16)	89.11(9)
O5-M-N1	91.57(15)	91.00(11)	90.89(9)	90.29(16)	90.89(9)
N1-M-N1^{i}	180.0	180.0	180.0	180.0	180.0
O5^{i}-M-O1^{i}	87.08(15)	88.60(11)	88.74(9)	89.67(14)	88.91(9)
O5-M-O1^{i}	92.92(15)	91.40(11)	91.26(9)	90.33(14)	91.09(9)
O1^{i}-M-N1^{i}	73.93(13)	75.50(10)	76.91(8)	78.77(13)	77.30(8)
O1^{i}-M-N1	106.07(13)	104.50(10)	103.09(8)	101.23(13)	102.70(8)
O5^{i}-M-O1	92.92(15)	91.40(11)	91.26(9)	90.33(14)	91.09(9)
O5-M-O1	87.08(15)	88.60(11)	88.74(9)	89.67(15)	88.91(9)
O1-M-N1^{i}	106.07(13)	104.50(10)	103.09(8)	101.23(13)	102.70(8)
O1-M-N1	73.93(13)	75.50(10)	76.91(8)	78.77(13)	77.30(8)
O1-M-O1^{i}	180.0	180.0	180.0	180.0	180.0

[a] Symmetry transformations used to generate equivalent atoms: i $-x$, $-y+1$, $-z$.

Table 2. Selected bond lengths [Å] and angles [°] for **6**.[a]

Co1−O8^{i}	2.071(2)	O7−C10	1.244(4)
Co1−O1	2.087(2)	O8−C10	1.263(4)
Co1−N1	2.109(2)	O8−Co1^{i}	2.071(2)
Co1−N7	2.146(3)	N1−N2	1.338(3)
Co1−N6	2.161(3)	N1−C2	1.341(4)
Co1−N5	2.167(3)	N2−C4	1.356(4)
Co2−O4	2.052(2)	N3−N4	1.338(3)
Co2−N3	2.097(3)	N3−C7	1.341(4)
Co2−O5	2.108(2)	N4−C9	1.352(4)
Co2−N10	2.135(3)	C1−C2	1.496(4)
Co2−N9	2.178(3)	C2−C3	1.399(4)
Co2−N8	2.184(3)	C3−C4	1.377(4)
O1−C1	1.277(4)	C4−C5	1.489(4)
O2−C1	1.234(4)	C6−C7	1.489(4)
O3−C5	1.243(4)	C7−C8	1.395(4)
O4−C5	1.261(4)	C8−C9	1.380(4)
O5−C6	1.271(4)	C9−C10	1.488(4)
O6−C6	1.247(4)		
O8^{i}-Co1-O1	175.81(8)	O4-Co2-N3	100.89(10)
O8^{i}-Co1-N1	98.46(9)	O4-Co2-O5	177.94(9)
O1-Co1-N1	77.52(9)	N3-Co2-O5	77.10(9)
O8^{i}-Co1-N7	92.06(9)	O4-Co2-N10	89.00(10)
O1-Co1-N7	91.99(9)	N3-Co2-N10	170.06(11)
N1-Co1-N7	169.38(10)	O5-Co2-N10	93.01(10)
O8^{i}-Co1-N6	89.34(10)	O4-Co2-N9	90.40(12)
O1-Co1-N6	89.42(10)	N3-Co2-N9	89.13(12)
N1-Co1-N6	89.42(11)	O5-Co2-N9	89.11(11)
N7-Co1-N6	92.15(11)	N10-Co2-N9	91.77(12)
O8^{i}-Co1-N5	89.28(10)	O4-Co2-N8	90.58(12)
O1-Co1-N5	91.85(10)	N3-Co2-N8	90.89(12)
N1-Co1-N5	89.20(11)	O5-Co2-N8	89.92(11)
N7-Co1-N5	89.50(11)	N10-Co2-N8	88.04(13)
N6-Co1-N5	177.94(9)	N9-Co2-N8	179.00(12)

[a] Symmetry transformations used to generate equivalent atoms: i $-x+1$, $-y+1$, $-z+1$.

Similar results were obtained for **1**, **4**, and **5** and are tabulated in Table 4.

Some unique and intriguing phenomena were observed upon heating of **1**–**5**. Figure 3a shows the PXRD pattern of **3** before heating. After heating it under an inert atmosphere to 230 °C, all four water molecules were dissociated from the sample and the color of the sample changed from the original beige to violet; this suggests a coordination and geometry change of the metal center from octahedral to tetrahedral.[14] The PXRD pattern taken at this point is also shown in Figure 3b, which clearly reflects that the crystal structure collapsed and the sample became *amorphous*. While the long-range order no longer exists, the local metal–pdc bonds remain and were confirmed by the strong characteristic absorption band for the asymmetric stretching of the carboxylate C=O seen in the FT-IR spectrum, which compared well with that taken before heating ($\nu_{as(C=O)} = 1640\,cm^{-1}$). The disappearance of the band at $\sim 3537\,cm^{-1}$, which corresponds to the vibration of the water O–H bonds, is also in full agreement with the observation of the water loss from TGA experiments (Table 4). After the amorphous sample was placed in the water for 30 minutes, its turned from violet back to the original beige, and the powder pattern taken at this

Table 3. Selected hydrogen bond lengths [Å] and angles [°] for **1**, **2**, **3**, **4**, and **5**.[a,b]

D–H···A	1	2	3	4	5
O4–H1···O2^{ii}	2.515(5)	2.512(3)	2.529(3)	2.521(5)	2.524(3)
	175.5	174.7	174.4	160.0	173.5
N2–H6···O6	2.713(6)	2.704(4)	2.707(3)	2.710(5)	2.709(3)
	160.7	158.6	157.4	163.0	166.3
O6–H5···O1^{i}	2.891(6)	2.825(4)	2.832(3)	2.801(5)	2.834(3)
	161.9	168.6	155.2	166.3	170.1
O6–H4···O3^{ii}	2.908(6)	2.921(4)	2.919(3)	2.935(5)	2.931(3)
	169.0	154.8	169.9	175.9	173.4
O5–H3···O2^{iii}	2.720(5)	2.703(4)	2.728(3)	2.731(5)	2.732(3)
inter–layer	163.1	156.6	160.6	145.3	165.7
O5–H2···O3^{iv}	2.886(5)	2.854(4)	2.855(3)	2.870(5)	2.874(3)
inter–layer	173.1	166.4	172.9	175.3	164.4

[a] Symmetry transformations used to generate equivalent atoms: i $-x, -y+1, -z$; ii $-x+1, y+1/2, -z+1/2$; iii $x, -y+1/2, z+1/2$; iv $x-1, y, z$. [b] Bond length = d(D···A); bond angle = ∢(DHA).

Table 4. TGA and FT-IR data on polycrystalline samples of **1**, **3**–**5**.[a]

	1	3	4	5
T range [°C][b]	90–190	90–220	110–230	80–200
weight-loss (obsd) [%][c]	16.8	16.4	16.5	16.2
weight-loss (calcd) [%][d]	16.5	16.3	16.3	16.1
color (before loss of $4H_2O$)	white	beige	powder blue	white
color (after loss of $4H_2O$)	white	violet	green-blue	white
state (before loss of $4H_2O$)	crystalline	crystalline	crystalline	crystalline
state (after loss of $4H_2O$)	amorphous	amorphous	amorphous	amorphous
residue (major, at 800 °C)	Mn	Co	Ni	Zn
$\nu_{as(C=O)}$ [cm^{-1}][e]	1653	1640	1645	1635
$\nu_{O\text{-}H(sh)}$ [cm^{-1}][e]	3548	3537	3541	3545

[a] No data listed for **2**. See ref. [8]. [b] Temperature range for the weight loss of four water molecules. [c] Observed percentage weight loss of four water molecules. [d] Calculated percentage weigh loss of four water molecules. [e] Observed absorption bands for carboxylate C=O (asymmetric stretch) and water O-H bonds.

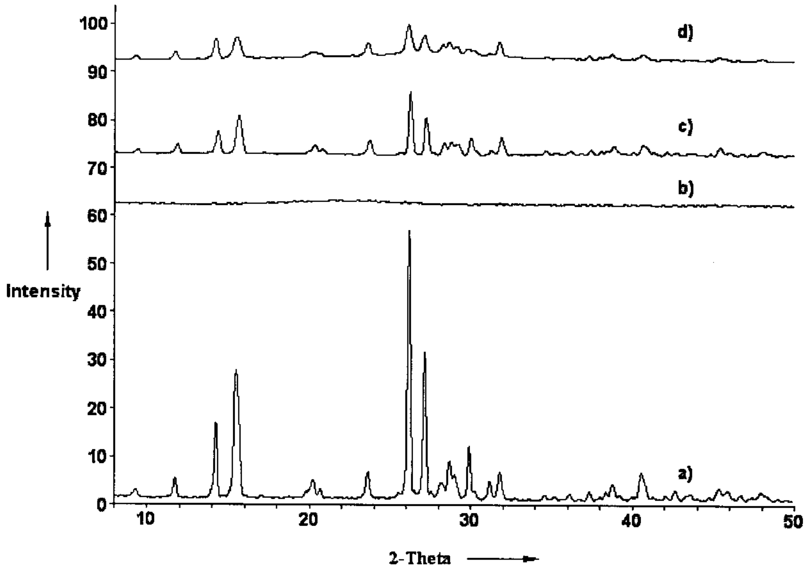

Figure 3. PXRD patterns for a) a single-phase polycrystalline sample of **3**; b) above sample after heated to 230 °C, at which point all four water molecules are dissociated and the sample color changed from beige to violet; c) sample in b) after placed in water for 30 minutes (the color turned back to beige); and d) sample after repeating the above procedure a)–c) five times.

stage (Figure 3c) is in excellent agreement with the original one shown in Figure 3a. The FT-IR spectrum also showed reappearance of a strong band at 3537 cm^{-1}, indicative of the returning of water molecules into the structure. Such a structure recovery process associated with a color change can be readily repeated through the simple heating–cooling cycles described above. Figure 3d gives the PXRD pattern taken after the same procedure was repeated five times on the original sample, indicating a very high reversibility. This reversible structure transformation involving a crystalline and an amorphous state was also observed for all other compounds. The observations are summarized in Table 4. Note that the cooling–heating (hydration–dehydration) cycles described here are different from the previously reported reversible structural transformation between two crystalline compounds.[15] In the case of the Ni compound (**4**), the process was also associated with a color change from powder blue (before water loss) to green bluish or aquamarine (after water loss). Evidently, the key to the observed phenomenon is the ability to break and reform the hydrogen-bonded network, which in turn results in the change in the metal coordination geometry.

The reactive intermediate [Co(H_2pdc)$_2$] and its reactions: The dehydrated [M(H_2pdc)$_2$] (M = Mn, Fe, Co, Ni, Zn) are highly reactive as they have unsaturated metal coordination sites. To probe the reactivity of these intermediate complexes, we selected [Co(H_2pdc)$_2$] as a reactive precursor for reactions with pyridine, a ligand that is similar in a number of ways to the water molecule. After being dissolved in methanol, pyridine was added to the solution. The reactions produced an interesting new compound **6**. An X-ray analysis on **6** revealed a unique "open-box" molecule[16] composed of four Co^{II} ions that form a square[17–18] and eight apical pyridine molecules (four above and four below the Co_4 plane), as shown in Figure 4a. The [Co_4(Hpdc)$_4$(py)$_{12}$] molecule is illustrated in Figure 4b with the carbon atoms of apical pyridines omitted for clarity. There are two types of crystallographically independent Co^{II} ions. Each Co1 is six-coordinate. In the equatorial plane, one Hpdc^{2-} forms a chelate bond with the metal through its carboxylate oxygen O1 and its adjacent pyrazole nitrogen N1, while the second Hpdc^{2-} uses its carboxylate oxygen O8 to form a monodentate bond with the metal (Co–O8^{i} = 2.071(2) Å). The remaining equatorial position is occupied by a pyridine nitrogen N7 with a Co–N bond length of 2.146(3) Å. The two pyridine molecules at the apical positions bond to the metal with Co1–N5 and Co1–N6

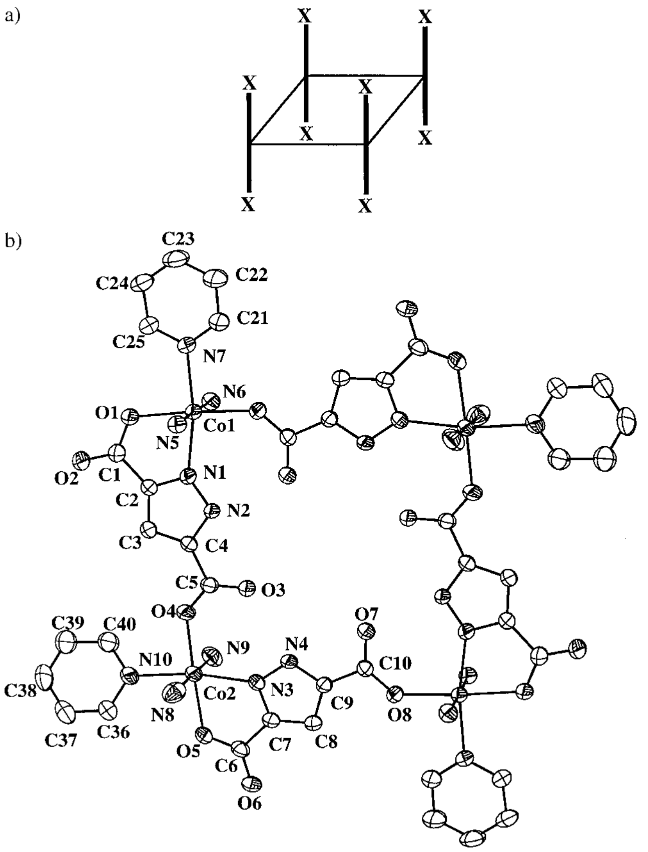

Figure 4. a) Schematic drawing representing a $\{Co_4(py)_8\}$ "open-box" molecule. X symbolizes a pyridine ring. b) The crystal structure of the $\{Co_4(Hpdc)_4\}$ square unit in **6** with the asymmetric unit labeled. Non-hydrogen atoms are shown and represented by thermal ellipsoids drawn at the 50% probability. Carbon atoms of the apical pyridines are omitted for clarity.

bond lengths of 2.167(3) and 2.161(3) Å, respectively. The acute angle (O1-Co1-N1) in the five-membered chelate ring is 77.52(9)°, and other angles around Co1 (O-Co1-O, O-Co1-N, and N-Co1-N) range from 89.28(10)–98.46(9)°.

The local coordination geometry around Co2 is very similar to Co1, with both axial positions taken by two pyridines with Co2–N8 and Co2–N9 bond lengths of 2.184(3) and 2.178(3) Å, respectively. The equatorial positions of Co2 are occupied by O5 and N3 in a chelating mode with Co2–O5 and Co2–N3 bond lengths of 2.108(2) and 2.097(3) Å, respectively. The carboxylate oxygen O4 coordinates to Co2 in a monodentate fashion with a Co2–O4 bond length of 2.052(2) Å. The bond angles around Co2 are similar to those of Co1. However, a notable difference lies in the relative orientation of the two axial pyridine rings bonded to the two metals. For Co2, the two pyridine rings make an angle of ~69.9°, whereas for Co1, they are approximately parallel (2.4°). Within a Co_4 square, each pair of neighboring Co1–Co2 atoms is bridged by a μ_3-Hpdc ligand. All pyrazole and pyridine rings at the equatorial positions are within the Co_4 plane. The metal–metal distances within a square are nearly identical (Co1–Co2 = 8.67 Å, Co1–Co2^i = 8.70 Å). The eight apical pyridine molecules are nearly perpendicular to the Co_4 square, with N5-Co1-N6 and N8-Co2-N9 angles of 177.94(9) and 179.00(12)°, respectively. A salient feature observed in this structure is the formation of a unique "open-box" by a Co_4 plane and the eight pyridines perpendicular to this plane (Figure 4a). Two guest pyridine molecules are encapsulated between every two adjacent boxes. The dihedral angles between these guest pyridine planes and the equatorial plane composed of four metals and four $Hpdc^{2-}$ ligands are 83.40° and 57.43°, respectively. Stacking of these "open-boxes" gives rise to a one-dimensional structure as shown in Figure 5. One group of apical pyridine rings bonded to Co1 is approximately parallel to a guest pyridine ring, which is encapsulated between the adjacent open boxes, with the pyridine–pyridine distance of ~3.5 Å that is highly subject to π–π interactions. Two kinds of hydrogen bonds exist inside the Co_4 square involving pyrazole nitrogen atoms (N2, N4) and the adjacent carboxylate oxygen atoms (O3, O7), giving N2–H4···O3 = 2.735 Å and N4–H5···O7 = 2.725 Å. The cross-section of the void in the square is 5.58 × 5.78 Å (distance between the two carboxylate oxygen atoms at the opposite sites, see Figure 4b). The dimensions of the box are estimated to be approximately 9.9 × 8.7 × 8.7 Å. Other guest species in **6** include another type of pyridine molecule located between the one-dimensional chains and the solvent molecules (MeOH and H_2O).

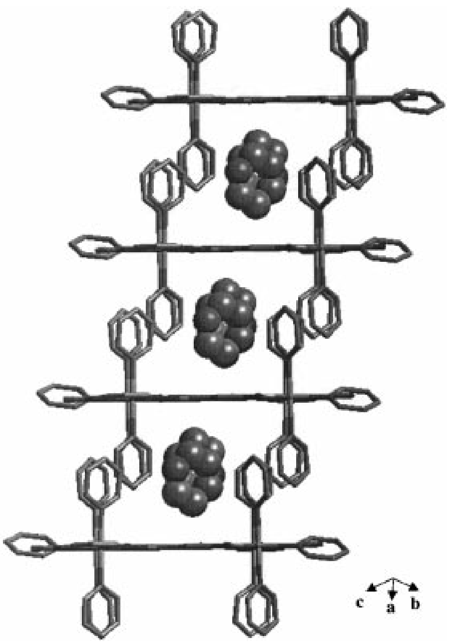

Figure 5. View along the *a* axis showing the stacking of the "open-box" molecules in **6**. The encapsulated pyridine guest molecules are also shown.

Conclusion

Hydrothermal reactions of transition metal salts (Mn, Fe, Co, Ni, Zn) with 3,5-pyrazoledicarboxylic acid have afforded a new family of coordination complexes with a parquet-patterned (basket-weave) structure held by hydrogen bonds. Upon hydration–dehydration, these compounds undergo a reversible structure interconversion process through a cooling–heating cycle. The process is associated with a distinct color change (Co, Ni, Fe). To the best of our knowledge, such a reversible structural interconversion between crystalline and amorphous states accompanied by color changes has not been previously reported. In addition, the dehydrated intermediate $[M(H_2pdc)_2]$ is highly unsaturated and can be used as a *reactive precursor* in the synthesis of new compounds with suitable ligands. An interesting open-box molecule containing a Co_4 square has been isolated. This compound can not be assembled by direct reactions of metal salts with the ligands. Continuing investigation of compounds of this type may be potentially important in the development of new indicators and sensors, and the continued use of reactive precursors may provide alternative routes to the assembly of interesting and unusual structures.

Experimental Section

Materials and instruments: Reagent grade $MnCl_2$, $Fe(NH_4)_2(SO_4)_2 \cdot 6H_2O$, $Co(NO_3)_2 \cdot 6H_2O$, $Ni(NO_3)_2 \cdot 6H_2O$, and $Zn(NO_3)_2 \cdot 6H_2O$ were purchased from Fisher and Alfa Aesar. 3,5-Pyrazoledicarboxylic acid monohydrate (97%) was purchased from Acros. All chemicals were used as received without further purification. Thermogravimetric analyses (TGA) were performed on a computer-controlled TA Instrument TGA 2050 system under nitrogen flow and with a scan rate of 5°C min^{-1}. Infrared spectra were measured from a photoacoustics Model 300 on a Bio-Rad FTS-6000 IR system. Powder X-ray diffraction (PXRD) experiments were performed on a Rigaku D/M-2200T automated diffraction system at an operating power of 40 kV/40 mA. The data were recorded at room temperature with a step size of 0.02 in 2θ and a scan speed of 1.7° min^{-1}. The analysis was carried out using JADE (windows) software package. The simulated powder patterns from single crystal data were generated for the phase identification. All hydrothermal reactions were performed in 23 mL Teflon-lined stainless steel bombs under autogenous pressure.

Synthesis of $[Mn(H_2pdc)_2(H_2O)_2] \cdot 2H_2O$ (1): Reaction of $MnCl_2$ (0.0315 g, 0.25 mmol), $H_3pdc \cdot H_2O$ (0.087 g, 0.5 mmol) and deionized water (10 mL) in the mole ratio of 1:2:2222 at 150°C for 3 days produced colorless column-like crystals of **1** in yield of 58.5% (0.064 g) based on Mn^{II}. The product was washed with water (3 × 10 mL) and acetone (3 × 10 mL), and dried in air. The final pH value was 1.5.

Synthesis of $[Fe(H_2pdc)_2(H_2O)_2] \cdot 2H_2O$ (2): Reaction of $Fe(NH_4)_2(SO_4)_2 \cdot 6H_2O$ (0.982 g, 0.25 mmol), $H_3pdc \cdot H_2O$ (0.087 g, 0.5 mmol), and deionized water (10 mL) in the mole ratio of 1:2:2222 at 150°C for 3 days yielded 0.062 g of products containing orange-yellow polyhedral crystals of **2** (~20%) and an unknown brown powder. The products were washed with water (3 × 10 mL) and acetone (3 × 10 mL), and dried in air. The final pH value was 2.0.

Synthesis of $[Co(H_2pdc)_2(H_2O)_2] \cdot 2H_2O$ (3): Reaction of $Co(NO_3)_2 \cdot 6H_2O$ (0.0728 g, 0.25 mmol), $H_3pdc \cdot H_2O$ (0.087 g, 0.5 mmol), and deionized water (10 mL) at 150°C for 3 days resulted in beige column-like crystals of **3** in high yield (88.8%, 0.098 g) based on Co^{II}. The product was washed with water (3 × 10 mL) and acetone (3 × 10 mL), and dried in air. The final pH value was 1.5.

Synthesis of $[Ni(H_2pdc)_2(H_2O)_2] \cdot 2H_2O$ (4): Reaction of $Ni(NO_3)_2 \cdot 6H_2O$ (0.0727 g, 0.25 mmol), $H_3pdc \cdot H_2O$ (0.087 g, 0.5 mmol), and deionized water (10 mL) in the mole ratio of 1:2:2222 at 150°C for 3 days resulted in powder blue column-like crystals of **4** in yield of 79.9% (0.088 g) based on Ni^{II}. The product was washed with water (3 × 10 mL) and acetone (3 × 10 mL), and dried in air. The final pH value was 1.5.

Synthesis of $[Zn(H_2pdc)_2(H_2O)_2] \cdot 2H_2O$ (5): Reaction of $Zn(NO_3)_2 \cdot 6H_2O$ (0.074 g, 0.25 mmol), $H_3pdc \cdot H_2O$ (0.087 g, 0.5 mmol), and deionized water (10 mL) in the mole ratio of 1:2:2222 at 150°C for 3 days generated colorless polyhedral crystals of **5** in yield of 49.4% (0.055 g) based on Zn^{II}. The product was washed with water (3 × 10 mL) and acetone (3 × 10 mL) and dried in air. The final pH value was 1.5.

Synthesis of $[Co_4(Hpdc)_4(py)_{12}] \cdot 4py \cdot 2H_2O \cdot 2CH_3OH$ (6): After heating compound **3** (51.89 mg) under nitrogen gas to remove the four water molecules, a violet powder of $[Co(H_2pdc)_2]$ (43.27 mg, calcd 43.43 mg) was collected. The $[Co(H_2pdc)_2]$ powder (6 mg) was dissolved in methanol (3 mL) in a vial to give a pale pink solution. Pyridine (2.0 mL) was then

Table 5. Crystallographic data, details of the data collection and structure refinement for **1**, **2**, **3**, **4**, **5**, and **6**.

	1	**2**	**3**	**4**	**5**	**6**
formula	$C_{10}H_{14}MnN_4O_{12}$	$C_{10}H_{14}FeN_4O_{12}$	$C_{10}H_{14}CoN_4O_{12}$	$C_{10}H_{14}NiN_4O_{12}$	$C_{10}H_{14}ZnN_4O_{12}$	$C_{102}H_{100}Co_4N_{24}O_{20}$
M_r	437.19	438.10	441.18	440.96	447.62	2217.78
crystal system	monoclinic	monoclinic	monoclinic	monoclinic	monoclinic	monoclinic
space group	$P2_1/c$ (No.14)	$P2_1/c$ (No.14)	$P2_1/c$ (No.14)	$P2_1/c$ (No.14	$P2_1/c$ (No.14)	$P2_1/c$ (No.14)
a [Å]	10.186(2)	10.023(2)	9.981(2)	9.896(2)	10.001(2)	9.9617(1)
b [Å]	12.473(2)	12.432(2)	12.426(2)	12.402(3)	12.430(2)	18.5080(2)
c [Å]	6.831(1)	6.813(1)	6.807(1)	6.810(1)	6.834(1)	28.4786(3)
β [°]	108.80(3)	108.42(3)	108.23(3)	108.15(3)	108.32(3)	93.076(1)
V [Å^3]	821.6(2)	805.4(2)	801.9(2)	794.2(2)	806.5(2)	5243.07(10)
Z	2	2	2	2	2	2
ρ_{calcd} [g cm^{-3}]	1.767	1.806	1.827	1.844	1.843	1.405
μ [mm^{-1}]	0.879	1.014	1.148	1.300	1.600	0.702
crystal size	0.15 × 0.10 × 0.10	0.18 × 0.15 × 0.08	0.45 × 0.18 × 0.15	0.16 × 0.06 × 0.03	0.20 × 0.18 × 0.15	0.48 × 0.18 × 0.12
T [K]	293(2)	293(2)	293(2)	293(2)	293(2)	220(2)
λ [Å]	0.71073	0.71073	0.71073	0.71073	0.71073	0.71069
θ range [°]	2.11–26.00	2.14–26.01	2.15–25.99	2.17–25.98	2.15–25.97	2.56–25.35
scan mode	ω-2θ	ω-2θ	ω-2θ	ω	ω-2θ	image plate ϕ oscillations
absorption type	Ψ scan	Ψ scan	Ψ scan	Ψ scan	Ψ scan	none
min/max transmissions	0.948/1.000	0.962/0.999	0.892/1.000	0.827/1.000	0.933/1.000	none
reflections collected	1748	1710	1705	1692	1711	32290
independent reflections (Rint)	1618 (0.0345)	1582 (0.0574)	1577 (0.0368)	1565 (0.0385)	1583 (0.0155)	9344 (0.0408)
observed reflections [$I > 2\sigma(I)$]	1114	1220	1307	1090	1290	8274
parameters	125	125	125	125	125	678
$R1$ [$I > 2\sigma(I)$][a]	0.0542	0.0426	0.0468	0.0500	0.0303	0.0595
$wR2$[b]	0.1093	0.0863	0.0752	0.0929	0.0649	0.1074
GOF	1.19	1.19	1.06	1.13	1.08	1.11
residual peak/hole [e Å^{-3}]	0.49/-0.44	0.89/-0.46	0.50/-0.30	1.18/-0.45	0.52/-0.37	0.41/-0.43

[a] $R1 = \Sigma||F_o| - |F_c||/\Sigma|F_o|$. [b] $wR2 = [\Sigma[w(|F_o^2| - |F_c^2|)^2]/\Sigma w(F_o^2)^2]^{1/2}$. Weighting: **1**, $w = 1/\sigma^2[F_o^2 + 2.80P]$, where $P = (F_o^2 + 2F_c^2)/3$; **2**, $w = 1/\sigma^2(F_o^2 + 1.80P)$; **3**, $w = 1/\sigma^2(F_o^2 + 1.80P)$; **4**, $w = 1/\sigma^2[F_o^2 + 3.0P]$; **5**, $w = 1/\sigma^2[F_o^2 + 1.50P]$; **6**, $w = 1/\sigma^2[F_o^2 + (0.02p)^2 + 10.0P]$.

0947-6539/01/0720-4436 $ 17.50+.50/0

added to the open vial. The color of the solution changed to red-pink. Orange-pink needle crystals of **6** (yield: ~25%) were formed after a slow evaporation of the solution for several days.

X-ray crystallography: Single-crystal structure analyses for compounds **1**–**5** were performed on an automated Enraf-Nonius CAD4 diffractometer equipped with graphite monochromatic $\mathrm{Mo_{K\alpha}}$ radiation. Lattice parameters were obtained from least-squares analyses of 25 computer-centered reflections with $6.55 \leq \theta \leq 13.93°$ (**1**), $5.98 \leq \theta \leq 13.46°$ (**2**), $9.24 \leq \theta \leq 14.73°$ (**3**), $6.20 \leq \theta \leq 14.42°$ (**4**), and $8.15 \leq \theta \leq 14.76°$ (**5**). The data collections for all crystals were monitored by three standard reflections every four hours. No decay was observed except the statistic fluctuation. Data collections were controlled by the CAD4/PC,[19a] the XCAD4-PC[19b] was used for data reduction. The crystal structure of **6** was determined by single-crystal X-ray diffraction analysis on an Rigaku R-AXIS IIc area detector employing graphite monochromatic $\mathrm{Mo_{K\alpha}}$ radiation. Indexing was performed from a series of 1° oscillation images with exposures of 400 s per frame. Hemisphere of data were collected using 4° oscillation angles with exposures of 1500 s per frame and a crystal-to-detector distance of 82 mm. Oscillation images were processed by using bioteX.[20] Raw intensities were corrected for Lorentz and polarization effects. Direct phase determination and subsequent difference Fourier map synthesis yielded the positions of all nonhydrogen atoms, which were subjected to anisotropic refinement. Hydrogen atoms were located from the difference Fourier map, but were not refined; their thermal parameters were set equal to $1.2 \times U_{\mathrm{eq}}$ of the parent nonhydrogen atoms. The final full-matrix, least-squares refinement on F^2 was applied for all observed reflections $[I > 2\sigma(I)]$. All calculations were performed by using the SHELX97 software package.[21] Analytic expressions of atomic scattering factors were employed, and anomalous dispersion corrections were incorporated.[22] Crystal data and details of the data collection and structure refinement for **1**–**6** are listed in Table 5.

Crystallographic data (excluding structure factors) for the structures reported in this paper have been deposited with the Cambridge Crystallographic Data Centre as supplementary publication no. CCDC- CCDC 160413 (**1**), CCDC 160414 (**2**), CCDC 160415 (**3**), CCDC 160416 (**4**), CCDC 160417 (**5**), and CCDC 160418 (**6**). Copies of the data can be obtained free of charge on application to CCDC, 12 Union Road, Cambridge CB21EZ, UK (fax: (+44)1223-336-033; e-mail: deposit@ccdc.cam.ac.uk).

Acknowledgements

The support of the National Science Foundation (DMR-9553066) and the REU supplemental funds are gratefully acknowledged.

---

[1] a) K. Miyamura, A. Mihara, T. Fujii, Y. Gohshi, Y. Ishii, *J. Am. Chem. Soc.* **1995**, *117*, 2377; b) *Comprehensive Supramolecular Chemistry, Vol. 10* (Eds.: J.-M. Lehn, J. L. Atwood, J. E. D. Davies, D. D. McNicol, F. Vögtle, D. N. Reinhoudt), Pergamon, Oxford, **1996**; c) M. Munakata, L. P. Wu, T. Kuroda-Sowa, M. Maekawa, Y. Suenaga, K. Furuichi, *J. Am. Chem. Soc.* **1996**, *118*, 3305.

[2] See, for example: a) G. R. Desiraju, *Crystal Engineering: The Design of organic Solids*, Elsevier, New York, **1989**; b) P. Brunet, M. Simard, J. D. Wuest, *J. Am. Chem. Soc.* **1997**, *119*, 2737; c) J. A. Swift, A. M. Pivovar, A. M. Reynolds, M. D. Ward, *J. Am. Chem. Soc.* **1998**, *120*, 5887; d) A. Ranganathan, V. R. Pedireddi, C. N. R. Rao, *J. Am. Chem. Soc.* **1999**, *121*, 1752; e) T. Sawaki, T. Dewa, Y. Aoyama, *J. Am. Chem. Soc.* **1998**, *120*, 8539.

[3] a) D. Braga, F. Grepioni, J. J. Byrne, A. Wolf, *J. Chem. Soc. Chem. Commun.* **1995**, 1023; b) A. D. Burrows, C. Chan, M. M. Chowdhry, J. E. McGrady, D. Michael, P. Mingos, *J. Chem. Soc. Rev.* **1995**, 329; c) C. B. Aakeröy, A. M. Beatty, *Chem. Chmmun.* **1998**, 1067; d) H. J. Choi, M. P. Suh, *J. Am. Soc. Chem.* **1998**, *120*, 10622.

[4] a) L. Pan, X.-Y. Huang, J. Li, Y. G. Wu, N.-W. Zheng, *Angew. Chem.* **2000**, *112*, 537; *Angew. Chem. Int. Ed.* **2000**, *39*, 527; b) L. Pan, X.-Y. Huang, J. Li, *J. Solid State. Chem.* **2000**, *152*, 236.

[5] a) L. Pan, N. Ching, X.-Y. Huang, J. Li, *Inorg. Chem.* **2000**, *39*, 5333; b) L. Pan, N. Ching, X.-Y. Huang, J. Li, *Inorg. Chem.* **2001**, *41*, 1271.

[6] A. Mayr, L.-F. Mao, *Inorg. Chem.* **1998**, *37* 5776.

[7] Y.-B. Dong, M. D. Smith, H.-C. zur Loye, *Solid State Sci.* **2000**, *2*, 861.

[8] J. Y. Lu, M. A. Lawandy, J. Li, T. Yuen, C. L. Lin, *Inorg. Chem.* **1999**, *38*, 2695.

[9] S. C. Chang, J. K. H. Ma, J. T. Wang, N. C. Li, *J. Coord. Chem.* **1972**, *2*, 31.

[10] B. Mernari, F. Abraham, M. Lagrenee, *Adv. Mater. Res.* **1994**, *1–2*, 317.

[11] a) M. A. S. Goher, A. A. Youssef, Z.-Y. Zhou, T. C. W. Mak, *Polyhedron* **1993**, *12*, 1871; b) R. V. Thundathil, E. M. Holt, S. L. Holt, K. J. Katson, *J. Chem. Soc. Dalton Trans.* **1976**, 1438; c) I. N. Pdyakova, T. N. Polynova, M. A. Porai-Khshits, *Koord. Khim.* **1981**, *7*, 1894; d) P. Richard, D. T. Qui, E. G. Bertaut, *Acta Crystallogr. Sect. B* **1974**, *30*, 628.

[12] A similar covalent bonded parquet network has been reported by Y. B. Dong, R. C. Layland, N. G. Pschirer, M. D. Smith, U. H. F. Bunz, H. C. zur Loye, *Chem. Mater.* **1999**, *11*, 1413.

[13] J. Bernstein, R. E. Davis, L. Shimoni, N. Chang, *Angew. Chem.* **1995**, *107*, 1689; *Angew. Chem. Int. Ed. Engl.* **1995**, *34*, 1555; a graph set $\mathrm{R}_d^a(n)$ stands for a pattern formed through hydrogen bonding, in which R specifies a ring, *a* and *d* are the numbers of hydrogen-bond acceptors and donors, respectively, and *n* is the number of atoms in the ring.

[14] J. D. Lee, *Concise Inorganic Chemistry*, 4th ed., Chapman & Hall, New York, **1991**.

[15] a) V. Kiritsis, A. Michaelides, S. Skoulika, S. Golhen, L. Ouahab, *Inorg. Chem.* **1998**, *37*, 3407; b) K. Endo, T. Sawaki, M. Koyanagi, K. Kobayashi, H. Masuda, Y. Aoyama, *J. Am. Chem. Soc.* **1995**, *117*, 8341.

[16] a) M. J. Hannon, C. L. Painting, W. Errington, *J. Chem. Soc. Chem. Commun.* **1993**, 307; b) R.-D. Schnebeck, E. Freisinger, B. Lippert, *Eur. J. Inorg. Chem.* **2000**, 1193.

[17] S. Leininger, B. Olenyuk, P. Stang, *Chem. Rev.* **2000**, *100*, 853.

[18] M. Fujita, K. Umemoto, M. Yoshizawa, N. Fujita, T. Kusukawa, K. Biradha, *Chem. Commun.* **2001**, 509.

[19] a) Enraf-Nonius CAD4-PC Software, Version 1.1, Enraf-Nonius, Delft (The Netherlands), **1992**; b) K. Hrams, XCAD4, Program for the reduction of CAD4 Diffractometer Data, University of Marburg (Germany), **1997**.

[20] BioteX: a suite of programs for the collection, redution and interpretation of imaging plate data, Molecular Structure Corporation, **1995**.

[21] G. M. Sheldrick, SHELX-97, Program for Structure Refinement, University of Göttingen (Germany), **1997**.

[22] *International Tables for X-ray Crystallography*, *Vol. C*, Kluwer Academic, Dordrecht, **1989**, Tables 4.2.6.8 and 6.1.1.4.

Received: March 26, 2001 [F3150]